



A LETTERS JOURNAL EXPLORING
THE FRONTIERS OF PHYSICS

OFFPRINT

**Topological changes at the gel transition of a
reversible polymeric network**

J. BILLEN, M. WILSON, A. RABINOVITCH and A. R. C. BALJON

EPL, **87** (2009) 68003

Please visit the new website
www.epljournal.org

TAKE A LOOK AT THE NEW EPL

Europhysics Letters (EPL) has a new online home at
www.epjjournal.org



Take a look for the latest journal news and information on:

- reading the latest articles, free!
- receiving free e-mail alerts
- submitting your work to EPL

www.epjjournal.org

Topological changes at the gel transition of a reversible polymeric network

J. BILLEN¹, M. WILSON¹, A. RABINOVITCH² and A. R. C. BALJON^{1(a)}

¹ *Department of Physics, San Diego State University - San Diego, CA 92128, USA*

² *Department of Physics, Ben-Gurion University of the Negev - Beer-Sheva, 84105, Israel*

received 19 May 2009; accepted in final form 9 September 2009

published online 8 October 2009

PACS 89.75.Fb – Structures and organization in complex systems

PACS 83.80.Qr – Surfactant and micellar systems, associated polymers

PACS 82.70.Gg – Gels and sols

Abstract – We investigate how the network topology of an ensemble of telechelic polymers changes with temperature. The telechelic polymers serve as “links” between “nodes”, which consist of aggregates of their associating end groups. Our analysis shows that the degree distribution of the system is bimodal and consists of two Poissonian distributions with different average degrees. The number of nodes in each of them as well as the distribution of links depend on temperature. By comparing the eigenvalue spectra of the simulated gel networks with those of reconstructed networks, the most likely topology at each temperature is determined. Topological changes occur at the transition temperatures reported in our previous study (BALJON A. R. C. *et al.*, *J. Chem. Phys.*, **126** (2007) 044907). Below the micelle transition the topology can be described by a robust bimodal network in which superpeer nodes are linked among themselves and all peer nodes are linked only to superpeers. At even lower temperatures the peers completely disappear leaving a structure of interconnected superpeers.

Copyright © EPLA, 2009

Reversible polymeric gels contain networks of physically associating polymers. These are copolymers incorporating soluble fragments along with a small fraction of insoluble chemical groups or linkers, which strongly attract each other. Different chemical units may be used as linkers depending on the solvent, *e.g.*, hydrophobic fragments on water-soluble polymers in aqueous solutions, and ionic groups on ionomers in organic solvents. The linkers form stable aggregates, which serve as temporary junctions in the resulting network structure [1,2]. Associating polymers show interesting rheological behavior, *e.g.* shear thickening followed by shear thinning in steady shear flow. Moreover, a transition from a fluid “sol” state to a glassy “gel” state is obtained by increasing the polymer concentration or decreasing the temperature. Transitions can also be triggered by applying a shear stress. It has been argued that the slowdown in the dynamics of the system when approaching the gel transition is not exclusively due to the longer lifetime of the aggregates. Structural changes in the network are believed to be a factor too [3,4]. They occur at the micelle transition temperature. In a previous work [5] we argued that the micelle transition resembles

the jamming transition [6,7] in amorphous and glassy systems [8]. Below this transition temperature, the stress relaxation time strongly increases. Moreover, the system shows solid-like behavior when sheared and develops a yield stress. In this study, we obtain further insight into the self-organized jammed states below the micelle transition temperature.

To this end, we use graph theory to quantify the topology of a simulated gel network (SGN). Details of the simulations can be found in [5]. We will show that the topology changes as a function of temperature and point out differences above and below the micelle transition. All simulations are carried out on a system of 1000 telechelic polymer chains. Each chain contained 8 beads. Both end groups are linkers. Non-bonded interactions between the beads are modeled using a purely repulsive Lennard-Jones (LJ) potential. All quantities are expressed in terms of the parameters (σ, ϵ, τ) of this potential. Beads connected by the chain structure interact through a FENE potential. Beads at chain ends can form junctions. They are modeled by a FENE potential with the same parameters. The positions of the beads are updated in molecular-dynamics simulations using the aforementioned force-fields. Attempts to create and destroy junctions

^(a)E-mail: abaljon@mail.sdsu.edu

are Monte Carlo moves [9]. The probability of success depends on $\exp(-\Delta U/kT)$, where ΔU is the difference in energy between the old and new state. It equals the potential energy of a junction and hence is the sum of the FENE potential and a negative constant $U_{assoc} = -22$ that models a dissociation barrier. The temperature is controlled by coupling the simulation cell to a heat bath. At each temperature the system is equilibrated for at least 5000τ before structural properties are sampled. Data at the lower temperatures are all obtained starting from a well equilibrated configuration at $T = 1.5$. The system is then slowly cooled at a rate of 2.500τ per $\Delta T = -0.1$, in order to obtain the desired temperatures. Data obtained by cooling the system from different initial states at $T = 1.5$ are identical within statistical fluctuations. Moreover, the statistical averages of structural properties do not change appreciably over time, even though the system shows rich dynamics with individual aggregates dissolving and new ones forming. Aggregates of end groups form and their sizes increase as temperature decreases. At low temperatures the system undergoes a gel transition: due to the aggregates an extended network forms that prohibits flow. Since the density is approximately 30%, a glass transition, typically displayed in higher-density systems, is not observed.

Our previous study [5] has defined four characteristic temperatures for the gel transition. At low temperature the relaxation time as a function of temperature diverges either as a stretched exponential at $T_0 = 0.29$ or as a power-law at $T_c = 0.4$. Above $T_A = 0.75$ the dependence of relaxation time on temperature becomes of Arrhenius type. At the micelle transition temperature $T_m = 0.51$ the number of reversible bonds strongly increases and the specific heat peaks. Below T_m the overall structure of the reversible network changes and a peak in the micelle size distribution becomes visible [5,10]. Between T_m and T_0 collective modes of relaxation are still available to the system and cause a net flow over long time periods. In this letter we investigate the structure of the SGN and how it changes with temperature. To this end, we compare it with that of complex networks found elsewhere in nature [11]. A complex network can be described as a set of nodes with links in between. In the well-known Erdős-Rényi (ER) random network [11], every pair of nodes is linked with a probability p . The degree distribution of this network, which describes the number of links k per node, is Poissonian:

$$P(k) = \frac{\langle k \rangle^k e^{-\langle k \rangle}}{k!}. \quad (1)$$

The average degree $\langle k \rangle = Np = \frac{2l}{N}$, where l equals the number of links and N is the number of nodes. In order to compare the simulated gels to other complex networks, we call an aggregate of end-groups a node. A polymer chain is identified as a link (unless both ends belong to the same aggregate). In a recent paper by Wang *et al.* [12]

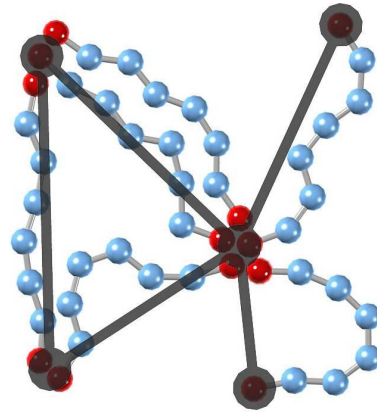


Fig. 1: (Color online) A 2D schematic illustrating the definition of nodes (black circles) and links (black lines) for a hypothetical bead-spring configuration. The beads at both chain ends are red and the others blue. Note that all simulations are performed in 3D.

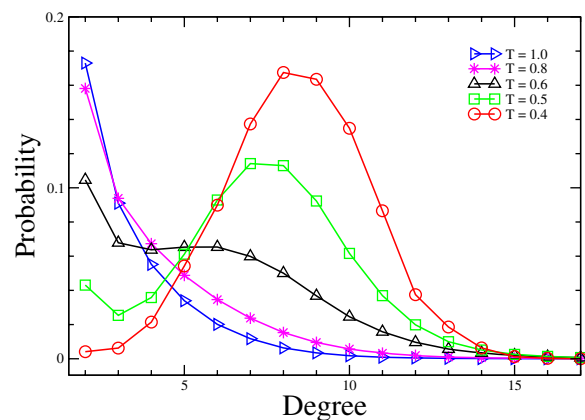


Fig. 2: (Color online) Degree distributions of the networks obtained from simulations at various temperatures.

a graph for reversible polymers was defined in the same way. In our simulations it is possible that the ends of more than one polymer chain connect the same pair of aggregates. If this is the case, we still count it as one link. A schematic picture illustrating the definition of a node and a link is shown in fig. 1. The degree distribution of the networks is shown in fig. 2. The probability distribution is bimodal and qualitatively similar to the aggregate distribution of the model at hand [5] and to that reported by others [10,13] for simulations of polymers with different chain lengths and interaction potentials. The goal of this study is to quantify the distribution and to characterize the topological changes using graph theory. As shown in fig. 3 for $T = 0.55$, a superposition of two Poisson distributions with different values of $\langle k \rangle$ fits the data,

$$P(k) = n_S \frac{\langle k \rangle_S^k e^{-\langle k \rangle_S}}{k!} + n_P \frac{\langle k \rangle_P^k e^{-\langle k \rangle_P}}{k!}. \quad (2)$$

Such a bimodal degree distribution is characteristic of complex networks which contain two types of nodes. Nodes

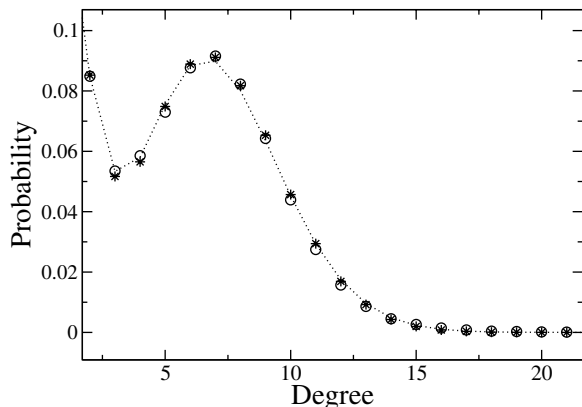


Fig. 3: Degree distribution for $T = 0.55$ (circles). The dotted line shows a fit to eq. (2) using the values in table 1. The asterisks result from a reconstruction of the gel network as described in the text.

in the distribution with the higher $\langle k \rangle$ value $\langle k \rangle_S$ are called “superpeers” (S), those in the other distribution “peers” (P) [14]. n_S and n_P are the fractions of superpeer and peer nodes, respectively. Within the simulations links break and new ones form all the time. In such a dynamic network, nodes alternate between being part of the superpeer and peer distribution.

Table 1 list the values of n_S , n_P , $\langle k \rangle_S$, and $\langle k \rangle_P$ of the fits to the SGN for a range of temperatures. With decreasing temperature n_S increases. Below $T = 0.4$ $n_P = 0$ and a single distribution of superpeers remains. The correlation coefficient (CC) of the fit is excellent at high temperatures, but becomes less accurate at temperatures below $T = 0.5$. We found that the single distribution below $T = 0.4$ has a slightly higher variance than predicted by a Poissonian model. Nevertheless, the data indicates that the SGN can be described by two Poissonians, whose relative contributions depend on temperature. This is shown in fig. 4, where the fraction of superpeer nodes n_S is plotted. The inset shows its rate of change. This rate peaks at the micelle transition ($T = 0.5$). At this temperature there is a strong increase in the average aggregate size. Moreover, the data in fig. 4 suggest that there is a qualitative change in the shape of their degree distribution and in the topology of the network structure.

To obtain further insight into these topological changes of the SGN with temperature, related networks (RN) were constructed according to the following recipe. At each temperature, we assign random coordinates in a 3D unit cell to N nodes maintaining the n_S/n_P ratio from table 1. Next, links are added in such a way that the desired values of $\langle k \rangle_S$ and $\langle k \rangle_P$ are obtained. To this end, the number of links between superpeers l_{SS} , the number of links between peers l_{PP} , and the number of links between a peer and a superpeer l_{PS} are chosen such that

$$\begin{aligned} \langle k \rangle_S &= (2l_{SS} + l_{PS})/n_S, \\ \langle k \rangle_P &= (l_{PS} + 2l_{PP})/n_P. \end{aligned} \quad (3)$$

Table 1: Results of fits of degree distributions to eq. (2).

T	n_S	n_P	$\langle k \rangle_S$	$\langle k \rangle_P$	CC
5.0	0.063	0.937	1.512	0.420	1.000
3.0	0.100	0.900	1.915	0.533	1.000
2.2	0.124	0.876	2.238	0.621	1.000
1.8	0.137	0.863	2.551	0.716	1.000
1.5	0.165	0.835	2.731	0.735	1.000
1.2	0.193	0.807	3.264	0.890	1.000
1.0	0.226	0.774	3.867	1.045	1.000
0.8	0.303	0.697	4.784	1.266	1.000
0.7	0.380	0.620	5.544	1.402	0.999
0.6	0.525	0.475	6.552	1.387	1.000
0.55	0.604	0.396	7.131	0.997	1.000
0.5	0.777	0.223	7.765	0.830	0.991
0.45	0.991	0.009	8.356	0.984	0.976
0.4	1.0	0.0	8.620		0.976
0.3	1.0	0.0	8.720		0.960

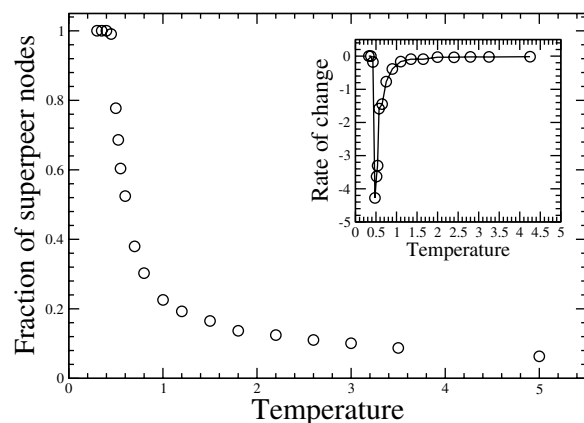


Fig. 4: Fraction of superpeers as a function of temperature. The inset shows the rate of change of the fraction of superpeers.

Initially, all links are chosen randomly. Further modifications are necessary given that the SGN is a spatial graph [11], because chain molecules that form the links have a finite size. They are approximately 7σ long when fully stretched. Hence we allow only links between nodes that are shorter than a certain cutoff distance. The number of each type of link and hence the values of $\langle k \rangle_S$ and $\langle k \rangle_P$ are unchanged. To decide on the value of the cutoff distance, we calculate clustering coefficients. For a particular node, the clustering coefficient is defined as the fraction of its neighbors that connect among themselves. The clustering coefficient of the entire network is obtained by averaging over all nodes of degree two and up [11]. Spatial dependence causes the clustering coefficient of a network to increase. Figure 5 shows the clustering coefficient as a function of temperature for the SGN (circles). It turns

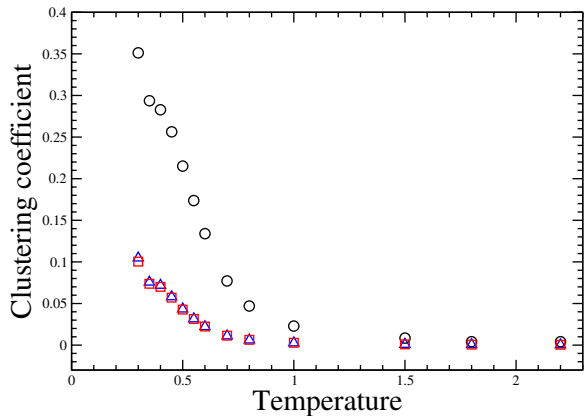


Fig. 5: (Color online) The clustering coefficient as a function of temperature. The circles are for the SGN. After rewiring the values change to those indicated by the blue triangles. The red squares are the calculated values from eq. (4).

out that the clustering coefficient of a graph with purely random links is much smaller than that of the SGN, as expected. A RN is constructed by adjusting the cutoff distance so as to match its clustering coefficient to that of the SGN. At $T = 0.55$ a cutoff distance of 0.28 is needed. Given the dimensions of our system this corresponds to 6.6σ . At higher T , the value of the cutoff distance slightly increases. The degree distributions of the RN are similar to that of the SGN (shown in fig. 3 for $T = 0.55$).

This finishes the description of the construction of the RN. To further explore the relation between the SGN and random graphs we have investigated what happens to the clustering coefficient of the SGN when spatial dependence is removed. This task is achieved through a rewiring process in which links of restricted length are replaced by ones with arbitrary length in such a way that the degree distribution is preserved¹. During rewiring, the clustering coefficient decreases. Its steady state values are shown in fig. 5 (triangles). Also shown is the theoretical value of the clustering coefficient [15] of an ER network with average degree $\langle k \rangle$:

$$C = \frac{\langle k \rangle}{N} \left[\frac{\langle k^2 \rangle - \langle k \rangle^2}{\langle k \rangle^2} \right]^2, \quad (4)$$

where N , the total number of nodes, is matched to that observed in the SGN. As one can see, the clustering coefficients of the rewired SGN are very close to those predicted by this equation.

We now further investigate the spatial dependent SGN using the RN for which the clustering coefficient was matched by restricting the length of allowed links. The network topology is quantified in more detail by the number of links and their distribution (l_{SS} , l_{PP} , and l_{PS}). There is still one degree of freedom in choosing these three numbers in such a way that eq. (3) is satisfied.

¹Starting with the configuration taken from the SGN, endpoints of two links are switched according to the following procedure: i) Randomly select links ℓ_{hi} and ℓ_{jk} connecting nodes n_h , n_i and n_j , n_k , respectively. ii) Remove links ℓ_{hi} and ℓ_{jk} , followed by the creation of new links ℓ_{hj} and ℓ_{ik} if none of these links already exist.

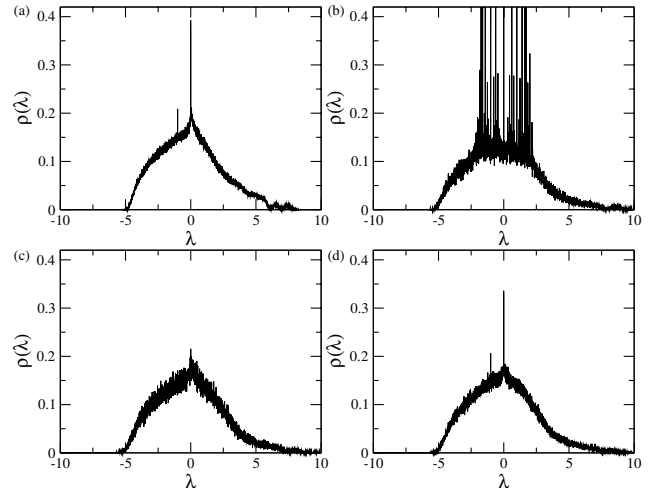


Fig. 6: A comparison of the spectral density of of the SGN (a) with RNs (b)–(d). In (b) the networks of peers and superpeers are disconnected ($l_{PS} = 0$), (c) is for the case that peers do not link among themselves ($l_{PP} = 0$), and (d) shows the RN that matches the SGN. In this case $l_{SS}/l_{tot} = 0.85 \pm 0.01$, $l_{PP}/l_{tot} = 0.02 \pm 0.01$, and $l_{PS}/l_{tot} = 0.13 \pm 0.01$.

Hence another property is needed to decide which link distributions best mimic the simulated gel networks. To this end, we calculate the spectral density $\rho(\lambda)$ of the adjacency matrix of a specific configuration of the SGN [16]:

$$\rho(\lambda) = \frac{1}{N} \sum_{j=1}^N \delta(\lambda - \lambda_j), \quad (5)$$

where the λ_j are the eigenvalues of the adjacency matrix. The results are averaged over 100 independent configurations of the SGN. The result is shown for $T = 0.55$ in fig. 6(a). The spectrum of the SGN is then compared with that of RNs for a range of choices for the number of links, chosen such that eq. (3) is satisfied. As seen in fig. 6, when $l_{PS} = 0$ and hence l_{PP} is maximum (b), the spectrum possesses many peaks. This is due to an abundance of disconnected clusters (groups of nodes linked together). The spectrum of a network in which $l_{PP} = 0$ and hence all peers are only connected to superpeers (c) is the smoothest. In all cases the spectrum is asymmetric. As we reported elsewhere [17], this is due to the spatial dependence of the network. Without spatial dependence, ER networks are symmetric in the limit $N \rightarrow \infty$. We use the height of the peak at $\lambda = -1$ as a criterion to determine the value of l_{PP} for which the RN spectrum best matches that of the SGN. As we show elsewhere [17], the height of this peak depends on the number of triangles. A triangle is a structure in which three links connect three nodes. An increase in l_{PP} leads to an increase in the number of triangles and hence in the peak height at $\lambda = -1$. The best match is shown in fig. 6(d). In this case $l_{SS}/l_{tot} = 0.85 \pm 0.01$, $l_{PP}/l_{tot} = 0.02 \pm 0.01$, and $l_{PS}/l_{tot} = 0.13 \pm 0.01$. Here $l_{tot} = l_{SS} + l_{PP} + l_{PS}$. We found that the fractions of the “giant network component” [11] in the SGN and RN at these settings are comparable as well.

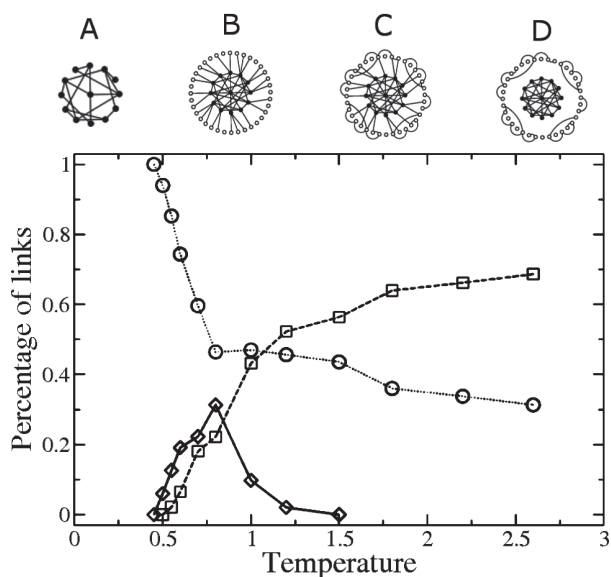


Fig. 7: Percentage of each type of link as a function of temperature. Circles for l_{SS}/l_{tot} , squares for l_{PP}/l_{tot} , and diamonds for l_{PS}/l_{tot} . Lines are guides for the eye. The cartoons show the transitions in the peer-superpeer networks. Superpeers are shown as closed dots and peers as open dots.

A similar comparison is performed for all temperatures. The results are shown in fig. 7. Sketches of the peer-superpeer network are displayed as well. At the highest temperatures the system consists of two separate networks (D). If the temperature is lowered, links between peers and superpeers are formed (C). Gradually the number of peers and the number of links in between them decrease. At $T = 0.5$ the number of links between peers vanishes and every peer is linked to a superpeer (B). Finally, below $T = 0.4$ only superpeers and links between them remain (A).

We conclude that during the transition from a fluid to a gel state the SGN undergoes several topological changes. These were studied by means of graph theory, considering aggregates as nodes and polymer chains as links. Construction of representative bimodal graphs (RN) has allowed us to investigate their topology in detail. Spatial effects were accounted for by restricting the size of links in such a way that the clustering coefficient of the RNs matches that of the SGNs. By comparing spectral densities, we were able to determine the number of links between peers and between superpeers, as well as those connecting peers to superpeers. We detected that significant changes in the topology occur at temperatures we have previously characterized [5] as transition temperatures. Most importantly, below the micelle transition temperature $T_m = 0.5$ links between the peers disappear. The resulting topology has been widely studied in the literature [18] and was shown to be extremely robust. Moreover, below $T_c = 0.4$ the peer nodes themselves disappear and a single degree distribution remains. Given that the topological changes occur at the same temperatures as the rheological transitions

observed in previous work [5], we believe that these effects could be intimately related. At low temperatures, flow can only occur when aggregates break into smaller parts. Depending on the network topology, simultaneous breakup of several aggregates might be necessary. Currently, we investigate the rates at which aggregates form and disappear and how these rates depend on aggregate size and system temperature. Knowledge of these rates will allow us to construct master equations for the evolution of the superpeer and peer populations.

The authors thank Dr R. V. D. HOFSTAD for helpful suggestions. This work was supported by a grant from the NSF under Grant No. DMR0517201.

REFERENCES

- [1] KUMAR S. K. and DOUGLAS J. F., *Phys. Rev. Lett.*, **87** (2001) 188301.
- [2] REGALADO E. J., SELB J. and CANDAU F., *Macromolecules*, **32** (1999) 8580.
- [3] CATES M. E. and WITTEN T. A., *Macromolecules*, **19** (1986) 732.
- [4] VACCARO A. and MARRUCCI G., *J. Non-Newtonian Fluid Mech.*, **92** (2000) 261.
- [5] BALJON A. R. C., FLYNN D. and KRAWZSENEK D., *J. Chem. Phys.*, **126** (2007) 044907.
- [6] O'HERN C. S., SILBERT L. E., LIU A. J. and NAGEL S. R., *Phys. Rev. E*, **68** (2003) 011306.
- [7] LIU A. J. and NAGEL S. R., *Jamming and Rheology: Constrained Dynamics at Microscopic and Macroscopic Scales* (Taylor & Francis, London) 2001.
- [8] DUDOWICZ J., FREED K. F. and DOUGLAS J. F., *J. Phys. Chem. B*, **109** (2005) 21350.
- [9] BALJON A. R. C., VORSELAARS J. and DEPUY T. J., *Macromolecules*, **37** (2004) 5800.
- [10] BEDROV D., SMITH G. D. and DOUGLAS J. F., *Europhys. Lett.*, **59** (2002) 384.
- [11] BOCALETTI S., LATORA V., MORENO Y., CHAVEZ M. and HWANG D.-U., *Phys. Rep.*, **424** (2006) 175.
- [12] BOHBOT-RAVIV Y., SNYDER T. M. and WANG Z.-G., *Langmuir*, **20** (2004) 7860.
- [13] KUMAR S. K. and PANAGIOTOPOULOS A. Z., *Phys. Rev. Lett.*, **82** (1999) 5060.
- [14] NEJDL W., WOLPERS M., SIBERSKI W., SCHMITZ C., SCHLOSSER M., BRUNKHORST I. and LOSER A., *Web Semant.*, **1** (2003) 177.
- [15] DAVIDSEN J., EBEL H. and BORNHOLDT S., *Phys. Rev. Lett.*, **88** (2002) 128701.
- [16] FARKAS I. J., DERENYI I., BARABASI A.-L. and VICSEK T., *Phys. Rev. E*, **64** (2001) 026704.
- [17] BILLEN J., WILSON M., BALJON A. R. C. and RABINOVITCH A., to be published in *Phys. Rev. E*.
- [18] TANIZAWA T., PAUL G., COHEN R., HAVLIN S. and STANLEY H. E., *Phys. Rev. E*, **71** (2005) 047101; VALENTE A. X. C. N., SARKAR A. and STONE H. A., *Phys. Rev. Lett.*, **92** (2004) 118702.